Dynamics of micelle formation from temperature-jump Monte Carlo simulations

G. Heinzelmann,* P. Seide Jr.,† and W. Figueiredo‡
Departamento de Fisica, Universidade Federal de Santa Catarina, 88040-900, Florianópolis, Santa Catarina, Brazil
(Received 29 July 2015; revised manuscript received 17 September 2015; published 6 November 2015)

In the present work we perform temperature jumps in a surfactant solution by means of Monte Carlo simulations, investigating the dynamics of micelle formation. We use a lattice model that allows orientational freedom and hydrogen bonding for solvent molecules, which can make a connection between the different time scales of hydrogen bond formation and amphiphilic aggregation. When we perform a large jump between a high-temperature nonmicellized state and a micellized state, there is strong hysteresis between the heating and cooling processes, the latter showing the formation of premicelles that act as nucleation centers for the assembly of larger aggregates and the former is a drive for dissociation of the existing aggregates. Hysteresis is not seen when we perform a small jump between two states that can be both micellized or nonmicellized. Looking for a more detailed analysis of the hydrophobic effect that drives aggregation, we compare the time evolution of the solvent hydrogen bonds in our system close and far from micelles and how that is affected by the formation of large clusters at low temperatures. We find a strong connection between them, with the total number of hydrogen bonds in the system always increasing when micelles are formed. To gain insights into the mechanism of premicellar formation and growth, we measure the lifetime of micellized amphiphiles as a function of the aggregate size and the stage of the aggregation process. Our results indicate that the premicelles are always unstable, quickly exchanging amphiphiles with the solution due to their low probabilty in equilibrium. Furthermore, we find that the stability of individual surfactants in micelles increases with the aggregate size, with the lifetime of amphiphiles in large micelles being as much as 35 times longer than in the case of the unstable premicellar region.

DOI: 10.1103/PhysRevE.92.052305 PACS number(s): 83.80.Qr, 87.15.ak, 87.15.nr

I. INTRODUCTION

Amphiphilic or surfactant molecules, defined by having regions with opposing dispositions towards the surrounding solvent [1], are capable of forming self-organized aggregates in solution such as bilayers, vesicles, and micelles [2,3]. They can be found in most of the domestic detergents and participate on the production and processing of several chemicals, such as fabric softeners, emulsifiers, pigments, and hydraulic fluids [4]. In water, the main force behind aggregation of surfactants is the hydrophobic effect, and their dual character (hydrophobic and hydrophilic) enables them to participate on a great number of biological processes [5]. At low amphiphilic concentrations, but above the so-called critical micelle concentration (CMC), they tend to form spherical micelles of different sizes. While the equilibrium properties of micellar solutions, like the size distribution and the CMC, are very important and the focus of many studies [6–12], the dynamics of micelle formation is essential to understand the underlying mechanism that drives self-aggregation. This mechanism can be investigated by performing concentration and temperature jump experiments, using different ionic and nonionic surfactants [13–18]. In such experiments, one applies a sudden change in the temperature or surfactant concentration and monitors the micelle behavior by measuring a property of the system, like conductivity, light scattering, fluorescence, or surface tension. Another approach is to perform an interfacial tension jump, as done by Lund *et al.* [19]. There PEP1-PEO20 amphiphiles were used, with the aggregation process triggered by quickly changing the solvent from DMF to a water-DMF mixture, and probed using small angle x-ray scattering (SAXS).

Searching for an accurate interpretation of the experimental data, several theoretical models for micelle formation have been proposed [20–27]. The most commonly found in the literature is the Aniansson and Wall (AW) mechanism [28,29]. According to this theory, the process of micelle formation is based on single-amphiphile exchange and can be divided into two relaxation times, one fast and other slow, which are related to the entering or exiting of individual surfactants from micelles and the formation or breakdown of entire aggregates, respectively. Even though other interpretations for these two relaxation times have been proposed, the AW formalism can successfully describe a number of experimental results [19,30–32]. In the case of the Lund *et al.* experiments with PEP1-PEO20 surfactants [19], the AW mechanism of single-amphiphile exchange can almost perfectly describe the micellar growth process after the interfacial tension jump performed on the system. Gottberg *et al.* [27] used stochastic dynamic simulations to obtain the exit rates of amphiphiles from micelles, as well as the free energy barriers for extraction or insertion of surfactant chains, obtained through the micellar dissociation rate constants and Kramers's rate theory. When including the exit rates obtained into the AW equations, there was good agreement with the simulation results, especially for shorter time periods associated with single-molecule insertion. Other experiments and theoretical models point to a possible third relaxation time of micellar formation, which can be ultrafast, ultraslow, or in between the fast and slow components. Photon correlation measurements by Trachimow *et al.* [17] have identified an ultraslow relaxation time caused by an excess of extra large micelles during equilibration and a later simulation study interpreted these results, also identifying

*germano.heinzelmann@posgrad.ufsc.br
†paulo.fsc@grad.ufsc.br
‡wagner.figueiredo@ufsc.br

a possible ultrafast relaxation time [24]. Danov *et al.* [20] have created a theoretical framework in which, in contrast to the AW model, the width of the micellar peak in the size distribution curve is not constant but varies during the micellization process. Three relaxation times were found, two of them coinciding with the AW theory, and another one in between these two that describes the variation in the width of the micellar size distribution.

Regardless of the model proposed, it is agreed that the force behind micellar aggregation in water is the hydrophobic effect, in which water tends to isolate hydrophobic species in order to maximize the number of hydrogen bonds and minimize the free energy ($H - TS$) of the system. The self-aggregation is more pronounced at lower temperatures and higher concentrations of amphiphiles, since it causes a decrease in the enthalpy (H) due to the hydrophobic effect, accompanied by a reduction in entropy that causes an increase in the entropic term scaled by the temperature ($-TS$). In the case of oil-water mixtures this ultimately leads to phase separation between the two species for higher oil concentrations. For amphiphiles this process is limited to mesoscopic domains, since the surfactant molecules have a chemical moiety that interacts favorably with water. It is therefore interesting to investigate the process of self-aggregation together with the hydrogen-bond dynamics of the aqueous solvent, which represents a challenge due to the disparity between the time scales involved in the two phenomena. All-atom molecular dynamics simulations, which can reproduce the water hydrogen bond (HB) formation or breakdown, are computationally expensive if one wants to obtain good sampling on the spontaneous aggregation process. Coarse-grained or lattice models, while successfully reproducing the dynamics of amphiphile aggregation, usually cannot account for the much faster time scales involved in the HB dynamics. In the past years, we have developed a body-centered cubic (BCC) lattice model for surfactant solutions that allows orientational freedom for the solvent molecules and the possibility of hydrogen bond formation or breakdown during the simulation [33–35]. We have used it to study the influence of different phases of the solvent in the equilibrium properties of micellar solutions and also in the orientational freedom of the solvent close to micelles and in the solvent bulk. More recently, we have employed it to analyze a temperature jump from a nonmicellized to a micellized state, obtaining the relaxation times of the process and comparing their behavior to the current theories available in the literature [36]. We found a strong connection between the HB dynamics of the system and the process of micellar formation, in which the solvent available surface area (SASA) of the micelles is reduced in order to maximize the number of solvent hydrogen bonds.

In the present work we consider the same model, a BCC lattice with single site solvent molecules and interconnected sites representing the amphiphiles. While in our previous study we focused on the relationship between the hydrogen bond dynamics of our system and the micellization process during one large jump, here we investigate the aggregation process in more detail by using different methods. First we perform different temperature jumps within nonmicellized and micellized regions and also a large jump from a nonmicellized to a micellized state. We show the evolution of the polydispersity curve during the temperature jump and how that relates to the current experiments and theories on the subject. We also use a set of correlation functions to study the effect of aggregate size on the single amphiphile exchange kinetics and the formation of premicelles before the system reaches an equilibrated micellized state. Similarly to Ref. [36], we also obtain the time evolution of the amphiphiles SASA and the hydrogen bonds of the solvent, making a connection between solvent interactions and the micellization process.

II. MODEL AND SIMULATIONS

Our micellar solution is defined as a BCC lattice, with each water molecule occupying one site in the lattice and the amphiphiles being represented as self-avoiding chains of connected sites. It is based on Larson's model, where the amphiphilic molecules are represented by interconnected sites on the lattice [37]. Here we consider a four-site flexible amphiphilic chain with three sites representing the hydrophobic tail and one site representing the hydrophilic head (H1T3). Our water molecules are modeled as having four bonding arms that are capable of forming hydrogen bonds (HBs) with their neighbors, depending on their orientation [33]. They can be in one of two states regarding their orientation, A or B, with the four arms forming a tetrahedral structure in each case, in an attempt to mimic the actual water molecule geometry. A hydrogen bond is formed when two arms from next-neighboring water molecules are pointing to each other (Fig. 1) and there is no HB formation between water and the amphiphiles. The system has no vacant sites, so all sites are occupied by either amphiphiles or water. When two water molecules form a hydrogen bond, the HB interaction energy between them is $\varepsilon = -2$. There is a repulsive interaction between all pairs of nearest-neighboring water molecules, working as an energetic penalty for nonbonded water molecules. We assume for this repulsive interaction energy the value $\varepsilon = 1$. For the other interactions in the system, we use a set of parameters that follows the usual definitions for lattice Monte Carlo simulations of surfactants in water and also provides both micellized and nonmicellized states in the range of temperatures considered. They are the following: $E_{HH} = 7\varepsilon$, $E_{HT} = 3\varepsilon$, $E_{HS} = -10\varepsilon$, $E_{SS} = 0$, $E_{TS} = -E_{TT} = \varepsilon$, where the subscripts read (S) for solvent

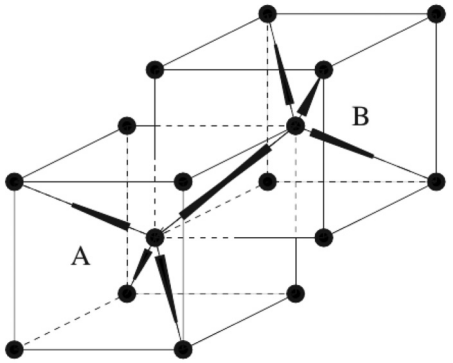

FIG. 1. The two possible states of the water molecules, A and B, and a hydrogen bond formed between them.

molecules, (T) for monomers in the hydrophobic tail, and (H) for the hydrophilic heads. The energy E_{HT}, for example, represents the interaction between a tail segment and a head segment.

Our simulations are carried out in the NVT ensemble, with a fixed volume fraction of amphiphiles of $\Phi = 0.05$. The linear size of the lattice is $L = 30$, which gives a total of $2L^3 = 54\,000$ sites in the BCC lattice. This yields a total of 675 surfactants in our solution, occupying 2700 sites and 51 300 water molecules. The temperature is measured in units of ε/k_B, where k_B is the Boltzmann constant, and we perform simulations in the temperature range between $T = 2.1$ and $T = 2.8$. Before we perform the temperature jumps, we equilibrate our systems at the initial temperatures, with the number of steps to reach equilibrium varying from 10^6 to 10^7 Monte Carlo steps (MCs). At the beginning of our equilibrium simulations, we randomly distribute, on an otherwise empty lattice, the amphiphiles and then the water molecules. The solvent molecules are distributed with a random orientation between the two possible states A and B. According to the Metropolis prescription [38], at each Monte Carlo step we randomly visit all of the solvent molecules and try to change their orientational state. After that, we attempt to move each surfactant through the usual reptation movement. Once the system is properly equilibrated, we perform the temperature jumps using the same Metropolis procedure at every step. For each jump we use at least 100 samples, in order to obtain a good ensemble of states and produce good averages. After the jump is performed, we are able to follow the evolution of the system properties until equilibrium is reached again at the new temperature. We analyze the evolution of the polydispersity curve, the number of hydrogen bonds in the system, the average number of amphiphiles per micelle, the concentration of free surfactants, and the solvent-accessible surface area (SASA) of the solute.

To investigate the stability of aggregates during equilibrium and through the temperature jumps, we also calculate a correlation function that measures the propensity of micellized amphiphiles to remain in that state in terms of their initial aggregate size, separating these sizes into small aggregates, premicelles, and full-grown micelles. This correlation function has the form:

$$C(t) = \frac{\langle X_M(t+\tau) X_{R_i}(\tau)\rangle}{\langle X_M(\tau) X_{R_i}(\tau)\rangle}, \qquad (1)$$

where the averages are over all the amphiphiles in every sample. $X_M(t)$ is the parameter that is going to label an amphiphile as micellized or not at time $t + \tau$ and $X_{R_i}(\tau)$ if the amphiphile is part of a particular size range i in the polydispersity curve at time τ. These ranges are defined according to the three regions of the polydispersity curve present in the AW theory. According to the latter, they can be divided into Regions I, II, and III. Region I contains only isolated amphiphiles and small aggregates, in our case also dimers and trimers (Fig. 2). Region III contains the local maximum in the polydispersity curve, with a Gaussian distribution of the highly populated region around this peak. Region II is in between Regions I and III and represents a section where few micelles are present in equilibrium. Nonetheless, Region II plays an important role when we perform a jump from a nonmicellized to a micellized state, since it contains the premicelles that are going to work as nucleation sites for the development of the fully grown micelles during equilibration. For $X_M(t)$, we give it a value of 1 if the molecule is part of an aggregate with at least two amphiphiles at time $t + \tau$ and 0 otherwise. We are looking for a continuous correlation, so $X_M(t)$ is always zero if it was not part of a micelle between times τ and $t + \tau$. The $X_{R_i}(\tau)$ values are assigned as 1 if the amphiphile is part of a micelle within the chosen range i and 0 otherwise. As explained before, these ranges follow the formalism of the AW theory and will be described in detail later under Results. We use different values for τ according to the stage of the temperature jump we want to analyze or if we perform this calculation in an equilibrated system.

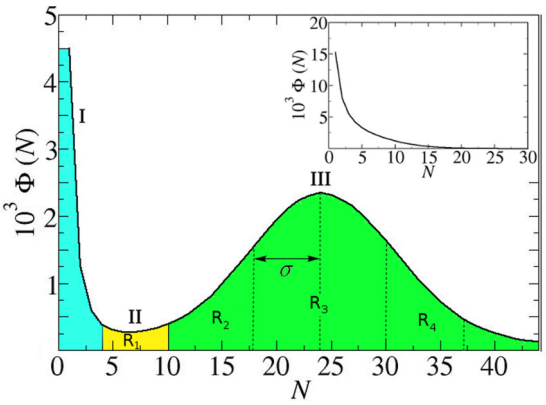

FIG. 2. (Color online) Micelle aggregate size distribution for $T = 2.2$, with the three regions from the AW theory, as well as the ranges in which we performed the correlation function calculations. The inset shows the same curve for $T = 2.8$, in which the solution is not micellized.

III. RESULTS AND DISCUSSION

To look at the dynamics of the micellization process, we perform heating and cooling jumps between a high-temperature state ($T = 2.8$) and a state with a much lower temperature ($T = 2.2$). The difference between the two is that the former does not have micelles, most amphiphiles being isolated or part of small transient aggregates without a peak in the size distribution (inset of Fig. 2). At $T = 2.2$, however, the system exhibits the properties of a micellized state (Fig. 2), with the three characteristic regions in the size distribution curve as described in the previous section. We perform both the forward and the backwards jumps, either cooling the system to $T = 2.2$ when it is equilibrated at $T = 2.8$ or vice versa, which corresponds to the heating process. The cooling process is able to reveal the dynamics of micelle formation as a function of time, so we can compare our results with theoretical and experimental studies on micellar aggregation. The heating process can provide interesting insights into the quick dissolution of micelles that takes place once we perform a sudden jump to a nonmicellized state. In Fig. 3 we show two three-dimensional plots, one for the heating [Fig. 3(a)] and another for the cooling process [Fig. 3(b)].

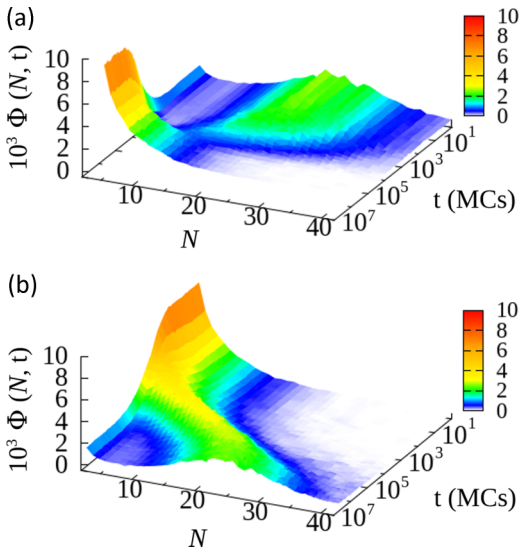

FIG. 3. (Color online) Three-dimensional plots showing the aggregate size distribution $\Phi(N,t)$ evolution with time after a heating (cooling) from (to) $T = 2.2$ to (from) $T = 2.8$, shown in (a) and (b), respectively. The process goes through distinct paths in the two cases, showing a strong hysteresis between the heating and cooling temperature jumps.

The coordinate axes are defined as the time in MCs (t), the aggregate size given by the number of amphiphiles per micelle ($N = \{1,2,3,\ldots\}$) and the volume fraction of a given micellar size as a function of time $\Phi(N,t)$. Since we are working in the NVT ensemble, the value of $\Phi(N)$ in equilibrium can also be seen as the relative probability of a given amphiphile to be in an aggregate of size N. We can immediately observe the strong hysteresis between the two transformations. During the heating process, the amphiphiles seem to dissociate directly from the aggregates located around the peak in the micelar distribution $\Phi(N)$ to the region of small aggregates, while the concentration of sizes between $N = 11$ and $N = 15$ remains nearly constant during the transformation. There are only small changes in Region II of the size distribution, with few amphiphiles occupying aggregates of intermediate sizes in the two temperatures and also during the heating process. The jump from $T = 2.8$ to $T = 2.2$, on the other hand, presents a very different picture. In this case we can clearly see the formation of intermediate aggregates, with the presence of a transient peak that is located at the local probability minimum for $T = 2.2$. This process is a clear indication of premicelle formation, which precedes the appearance of the larger aggregates that are predominant once equilibrium is reached. This mechanism can be directly compared to the experimental and theoretical results from Lund *et al.* [19], where a very similar path to equilibrium is obtained after a interfacial tension jump is performed. Their theoretical model follows the definitions from the AW theory, in which nucleation and micellar growth are governed by a mechanism of surfactant insertion or dissociation, and very good agreement is obtained with the experimental data. By plotting the evolution of the mean aggregation number P_{mean} with time, they have found that the best fit for this curve is a stretched exponential expression $P_{\text{mean}} = 1 - \exp[-(kt)^{\beta}]$. We use the

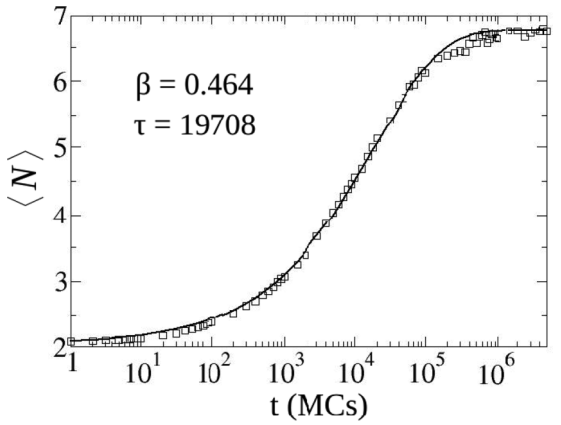

FIG. 4. Evolution of the mean aggregate size with time for a temperature jump between $T = 2.8$ and $T = 2.2$. The symbols are the results from our simulations and the line is the stretched exponential fit of the form $\langle N\rangle = \langle N\rangle_f - (\langle N\rangle_f - \langle N\rangle_i)\exp[-(t/\tau)^{\beta}]$, with the β and τ values also indicated.

same fit here, introducing a stretched exponential function of the form $\langle N\rangle = \langle N\rangle_f - (\langle N\rangle_f - \langle N\rangle_i)\exp[-(t/\tau)^{\beta}]$, where the angle brackets denote the average over all aggregates (or free amphiphiles in the case of $N = 1$) and the subscripts i and f the initial and final states of the system, respectively. As can be seen in Fig. 4, here the fit provides a value for β of 0.46, as opposed to 0.2 in the mentioned study. Still, there is good qualitative agreement between our model and the experimental and theoretical results from Ref. [19]. We also try to fit the mean aggregate size curve with two or three relaxation times in regular exponential expressions. Two relaxation times do not produce a good fit, and three relaxation times improve it but it is still inferior to the stretched exponential. In the case of the triple exponential fit we get a root-mean-square (RMS) relative error of 0.019 for the fitted N values and a correlation coefficient of 0.9994, whereas in the case of the stretched exponential we obtain 0.015 and 0.9995 for the same quantities. It should be mentioned that in this study we are analyzing nonequilibrium properties of micellar solutions using Monte Carlo steps, which makes it difficult to make a connection to real time as in the molecular dynamics simulations. Nevertheless, we are able to show that our model can qualitatively reproduce both experimental and theoretical aspects of micellar formation and therefore is worth being pursued further.

Due to the nature of our model, we can also measure a few other properties related to the aqueous solvent like HB formation and the evolution of the total solvent accessible surface area (SASA). In Fig. 5(a) we show the average number of hydrogen bonds per water molecule in our system in the first hydration shell of the surfactants in the solvent bulk, and also for all the water molecules in the system. The number of HBs in the bulk does not seem to be affected by the micellization process, since its increase occurs at a very short time scale and it stabilizes after that. On the other hand, the average number of hydrogen bonds in the first hydration shell has a local maximum, followed by a decrease for longer time periods. This decrease coincides with the formation of bigger micelles, which reduces the formation of water-water HBs in

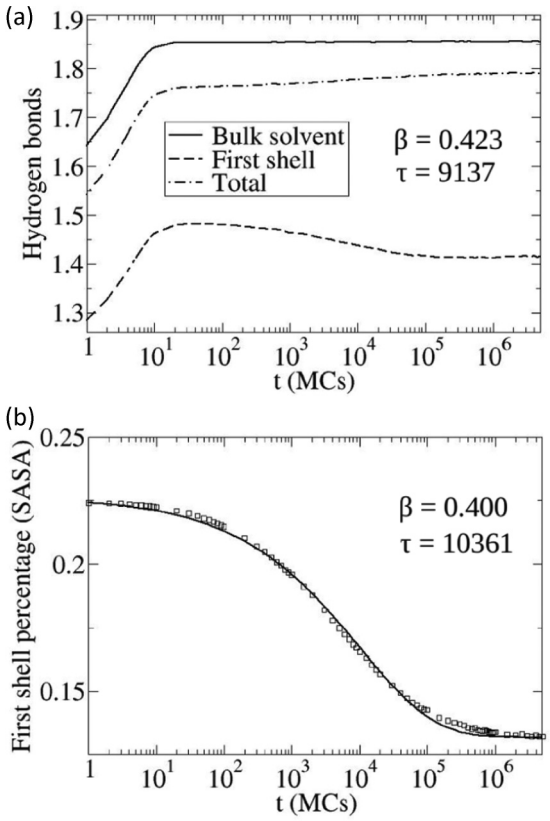

FIG. 5. (a) Average number of hydrogen bonds per water molecule in the solvent bulk (solid line), the first hydration shell (dashed line), and all the waters in the system (dash-dotted line). The graph shows a decrease in the average number of HBs for water molecules in the first hydration shell caused by micellization but an increase in the total number of HBs in the system in the same time interval. Also shown are the β and τ values obtained from the exponential fit of the time evolution of the number of HBs in the first hydration shell, using the equation $\langle n_{\rm HB}\rangle = \langle n_{\rm HB}\rangle_f - A_1\exp(-t/\tau_1) - (\langle n_{\rm HB}\rangle_f - \langle n_{\rm HB}\rangle_i - A_1)\exp[-(t/\tau)^\beta]$. (b) Evolution of the solvent accessible surface area of the solute (SASA), with the symbols representing the simulation results and the line the fit using the same expression of Fig. 4.

their vicinity. This is in agreement with the fact that water can isolate small nonpolar molecules without sacrificing hydrogen bonds, but that becomes harder as the nonpolar cavity increases in size, such as in the case of a large aggregate [39]. The average number of hydrogen bonds for all water molecules in the system shows the same initial increase as the bulk and first shell waters but is followed by a further increase when the system becomes micellized. This can be explained in terms of the evolution of the SASA, which we show in Fig. 5(b), calculated by dividing the number of water molecules in the first hydration shell of surfactants by the total number of water molecules in the system. The drop in the temperature causes the amphiphiles to aggregate due to the hydrophobic effect, which tends to maximize the total number of water HBs in the system by minimizing the SASA. This explains the second increase in the total number of water HBs that is triggered by the micellization process.

To test the connection between average micellar size (N), the number of HBs in the first hydration shell ($n_{\rm HB}$), and the SASA (S), we can also fit the time evolution of the last two properties to exponential expressions and obtain the relaxation times associated with the temperature jump. For the SASA we will use the stretched exponential expression $\langle S\rangle = \langle S\rangle_f - (\langle S\rangle_f - \langle S\rangle_i)\exp[-(t/\tau)^\beta]$, the same way we did with the average number of amphiphiles per micelle (N). For $n_{\rm HB}$, we will add to the stretched exponential a term that can account for the quick increase in the number of hydrogen bonds caused by the sudden decrease in temperature, which is not related to micellization, giving the equation $\langle n_{\rm HB}\rangle = \langle n_{\rm HB}\rangle_f - A_1\exp(-t/\tau_1) - (\langle n_{\rm HB}\rangle_f - \langle n_{\rm HB}\rangle_i - A_1)\exp[-(t/\tau)^\beta]$. In both cases we obtain a good fit, with a value of 0.0015 for the RMS relative error and 0.9991 for the correlation coefficient in the case of $n_{\rm HB}$. For the SASA (S), we get a value of 0.010 for the RMS relative error and 0.9992 for the correlation coefficient. Thus, we can make a direct comparison between the τ and β values obtained from the stretched exponential expressions of $\langle N\rangle$ and $\langle S\rangle$ and the τ and β values from the stretched exponential term of the $\langle n_{\rm HB}\rangle$ equation. As shown in Figs. 4 and 5, the corresponding values of β and τ are similar for the time evolution of all three properties, showing that they are intimately related and their change over time is a consequence of the micellization of the system. This result is consistent with the known mechanisms behind amphiphilic aggregation and its relation to the hydrophobic effect, even though we are using a simple model to investigate this phenomenon.

To compare the previous large perturbation to small temperature jumps, we have also performed two other transformations in our system. The first is a heating and cooling from temperature $T = 2.1$ to $T = 2.3$ and vice versa, both temperatures producing an equilibrium micellized state in our solution. The second is between two nonmicellized states, from $T = 2.6$ to $T = 2.8$ and vice versa. Figures 6 and 7 show the cooling and heating processes for these two transformations, respectively, using the same axes as in Fig. 3. Here we do not

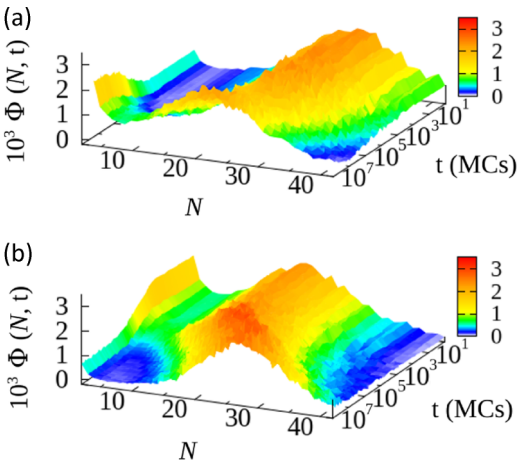

FIG. 6. (Color online) The same as in Fig. 3 but for (a) heating and (b) cooling jumps between 2.1 and 2.3. The solution is micellized in both cases, and the small temperature jump only causes shift in the polydispersity curve towards smaller or larger micelles.

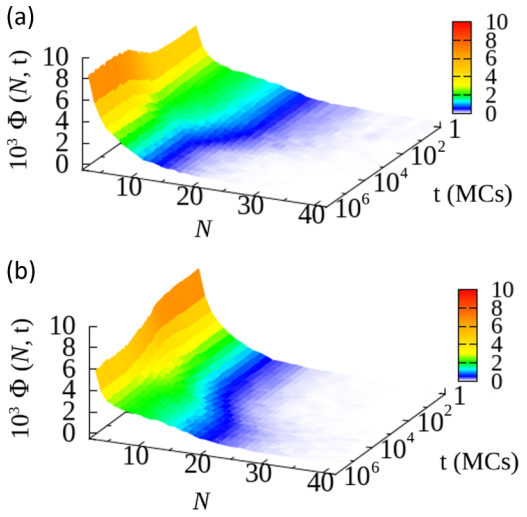

FIG. 7. (Color online) The same as Figs. 3 and 6, but for (a) heating and (b) cooling performed between temperatures $T = 2.6$ and $T = 2.8$. Here, also no hysteresis is observed between the two jumps, only a shift towards smaller or larger transient aggregates happening in a similar fashion.

identify the large difference between the heating and cooling for the two cases, since the hysteresis is small for both. It also seems to be mainly an exchange of surfactants between the already-existing aggregates in the case of the low-temperature jump and a small displacement towards larger or smaller transient aggregates in the case of the high-temperature jumps. In both cases the main characteristics of the system are conserved, and what we see is mainly a rearrangement of the amphiphiles towards the new equilibrium state without major changes in the solution. This is opposed to the case of the strong cooling we performed previously, where we can identify a process of nucleation followed by a period of micellar growth. We are going to analyze this process further by calculating the correlation times for different size ranges during the temperature jump and also during equilibrium.

Using the expression for the correlation described under Methods [Eq. (1)], we have calculated the propensity of amphiphiles to stay bound to micelles based on the aggregate size. The ranges R_i we have chosen are shown on the polydispersity graph of Fig. 2. Range 1 (R_1) is equivalent to Region II of the graph, with aggregates ranging from 4 to 10 amphiphiles per micelle. Range 3 (R_3) is located in the middle of the Gaussian distribution, within 1 σ from the peak on each side, which amounts to 18 to 30 amphiphiles per micelle. Ranges 2 and 4 are the values in the less-probable regions of the Gaussian distribution, being from 11 to 17 (R_2) and from 31 to 37 (R_4). Micelles from sizes 11 to 17 can also be seen as premicelles, which play an important role during the transition from a nonmicellized to a micellized state. The last range of values (R_4) accounts for large micelles, that take longest to form during micellization, as can be seen in Fig. 3(b). We calculate the correlation in three different stages of the cooling process from $T = 2.8$ to $T = 2.2$ to learn about the differences in the micellar dynamics at each step. As done in Ref. [26], we are going to define two variables, m and M, which are the size ranges in the minimum and maximum

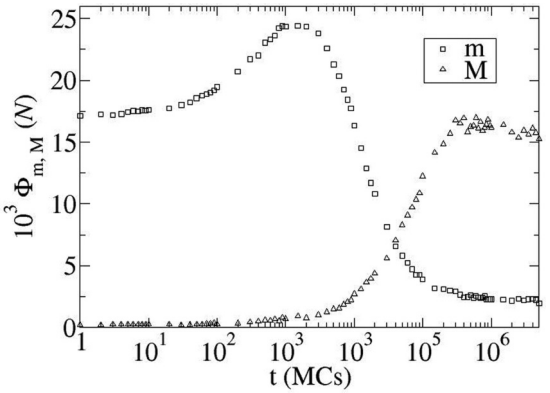

FIG. 8. Time evolution of the concentration of amphiphiles in aggregates that belong to the local minimum of the polydispersity curve (Region II), denoted as m, and the aggregates around the peak of the size distribution, denoted as M. Both of them show a peak around $t = 1000$ and $t = 300\,000$, respectively.

of the polydispersity curve of Fig. 2. M includes aggregates from sizes 21 to 27, and m has the same definition as R_2. By plotting the concentration of amphiphiles in the m and M regions as a function of time (Fig. 8), we notice that both of them produce a maximum during the micellization of the system from $T = 2.8$ to $T = 2.2$. The maximum occurs for m at $t_m = 1000$ and for M at $t_M = 300\,000$. Therefore, we decide to calculate the amphiphile correlation function starting from these two states at τ_m and τ_M, as well as in the equilibrated system at $T = 2.2$ (τ_e).

In Fig. 9(a) we show the correlation function for aggregates in the R_1 range for the three initial states described above. We can see that, regardless of the stage in the micellization process, the aggregates in Region II are short lived and are constantly exchanging amphiphiles with the solution. The fact that at time τ_m they represent a large part of the micelles in solution only slightly increases their long-term stability compared to τ_e and to τ_M. This is consistent with the low probability associated with the aggregates in Region II at $T = 2.2$ (Fig. 2), which indicates a higher free energy per surfactant molecule and a greater chance of amphiphile dissociation. This result shows that, instead of having a constant growth of the premicelles towards larger aggregates during micellization, which could be expected as an aggregation mechanism, the premicelles on Region II are unstable and form transient aggregates during the whole self-assembly process. In Fig. 9(b) we show the same correlation function but now for the other three ranges, R_2, R_3, and R_4. We do not show the $C_{R_4}(t)$ function for τ_m due to poor sampling of amphiphiles in this region, which does not produce a good curve. Here we have a different situation, with the correlation that starts at τ_m falling much more rapidly for all the ranges considered, followed by the correlation starting at τ_M and τ_e, respectively. The exception is $C_{R_2}(t)$, which has a very similar curve for the τ_M and τ_e initial states, most likely because this range is already equilibrated at τ_M [Fig. 3(b)]. The fact that the time correlations for ranges R_2 and R_3 starting from τ_m decay relatively quickly could also be attributed to the structure of these aggregates at this stage of the micellization process. They might not be fully developed and therefore show increased amphiphile dissociation compared

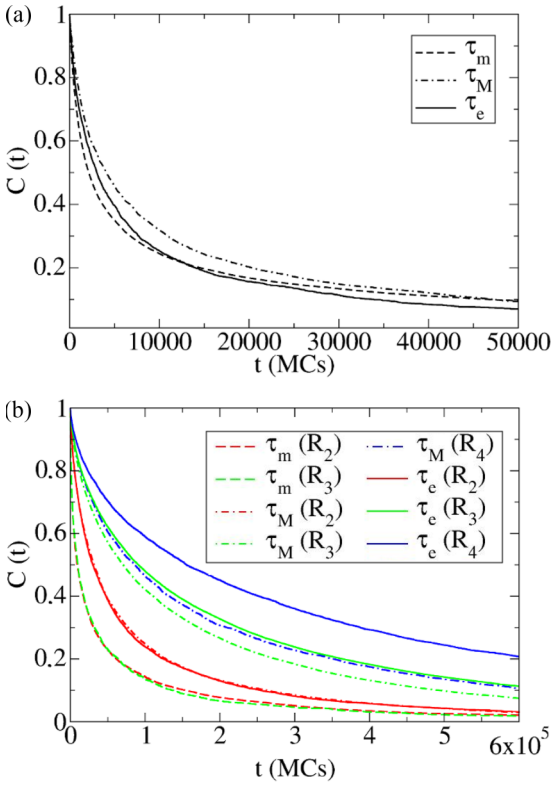

FIG. 9. (Color online) (a) Values for the correlation function [Eq. (1)] of aggregates between sizes 4 and 10 (R_1), which shows the propensity of amphiphiles to stay bound to micelles over time. For the initial times we used, τ_m, τ_M, and τ_e, the decay is similar, showing that these micelles are short lived regardless of the stage in the micellization process. (b) The same correlation function for the other three ranges (R_2, R_3, and R_4), in the three starting times of the previous item. The stability of micelles increases with the aggregate size and also with the proximity of the equilibrated state.

to the cases where we start at τ_M and τ_e. Unfortunately, we cannot make the same comparison for the R_4 range due the very small number of these aggregates appearing at $t = \tau_m$. As a general rule, we can see that the closer to equilibrium the more stable are the micelles from Region III and the smaller the tendency they have to dissociate. Also, for all starting times, the correlation increases with the micellar size, which was also observed at Ref. [25].

We can attempt to make a connection between the results from Fig. 9 and the hysteresis observed between the heating and cooling processes for the large jump. When the system is cooled, stable nucleation sites (Ranges R_2, R_3, and R_4) take longer to self-assemble due to the transient nature of the premicellar aggregates from Range R_1. Once that happens, the number of micelles is slowly reduced as their average size increases [Fig. 3(b)]. This process may also be accompanied by a structure change in the existing micelles, which increases their stability, as mentioned earlier when we looked at the time correlation of Ranges R_2 and R_3 starting from τ_m. When we heat the system, on the other hand, there is a cooperative dissolution of the large existing micelles and transient premicellar aggregates are not formed due to their low stability. Here, mainly due to the high temperature,

TABLE I. Amphiphile mean lifetimes as a function of the size ranges R_i. As shown in Fig. 9(b), there is a large increase in the residence time in micelles with the large sizes.

Size range	Average lifetime
R_1	5011
R_2	42876
R_3	115137
R_4	179351

amphiphiles go straight from micelles with sizes in Region III to free amphiphiles, dimers, and trimers (Region I). Therefore, a local maximum in the time evolution of the concentration of premicelles is not seen [Fig. 3(a)]. The temperature jumps performed between $T = 2.3$ and $T = 2.1$, which do not show hysteresis, do not present the m and M maxima in the cooling process, so the correlation for this jump cannot be calculated in the same way. Nevertheless, we believe that the residence times are closer to equilibrium during the cooling process, since we apply a much smaller perturbation in the system. Similarly to Ref. [25], we can also fit the initial decay of the four R_i curves of Fig. 9(b) in equilibrium to a single exponential function and calculate the rate of amphiphiles being lost to solution in each case. Even though the fit is not as good, we can roughly estimate the mean residence time of an amphiphile in a micelle as a function of the aggregate size, which we show in Table I. As expected, the lifetime of amphiphiles in micelles of Region II, equivalent to Range 1 (R_1), is much shorter than the others due to the instability of these micelles. The lifetime associated with Range R_1 is also in the same order of magnitude of the time scales involved in the time evolution of N, S, and n_{HB} during the cooling process from $T = 2.8$ to $T = 2.2$ (Figs. 4 and 5). This result further supports the idea that at least part of the aggregation process is a consequence of the dissolution of micelles in this size range, followed by the nucleation of amphiphiles in larger aggregates from Ranges R_2, R_3, and R_4. We can see that the average lifetime increases with micellar size, and for the largest set of sizes, between 31 and 37 surfactants per micelle, the mean lifetime is 35 times longer than the unstable micelles from the R_1 range. This is in disagreement with the original AW theory, which used the same value for the dissociation constant regardless of the aggregate size, but a similar behavior has also been observed in experiments with short surfactants of different lengths [40].

IV. CONCLUSIONS

In the present work we have used lattice Monte Carlo simulations to investigate the process of micellization of short amphiphiles by means of different temperature jumps applied on the system. In particular, we follow the transition between a nonmicellized and a micellized state and also between systems with similar features. We observe a large hysteresis when we compare the heating and cooling jumps between temperatures $T = 2.2$ and $T = 2.8$, and this is attributed to the formation of premicelles that happens when we reduce the system temperature. This behavior has been confirmed by several theoretical and experimental studies and is also consistent with the AW theory. We do not observe this hysteresis between

heating and cooling when we perform a jump between two states that are similar, only a small shift in the polydispersity curve of the existing aggregates for both jumps. In addition, we compare the formation of micelles to the hydrogen bond dynamics of the system, showing that the hydrophobic effect is the main force driving the aggregation of amphiphiles in the solution. This is counterbalanced by the reduction in entropy due to self-assembly, which in turn increases the free energy, especially for higher temperatures. Even though hydrogen bond formation with orientational freedom of water molecules is important for the investigation of surfactant self-assembly using our model, we do not believe that these features are the main causes behind the hysteresis observed. We plan on further testing that hypothesis by performing the same simulations without orientation-dependent water interactions and comparing the results, which will be the topic of future work.

To further investigate the dynamics of micellization during the cooling from a nonmicellized to a micellized state, we have also calculated the correlation function of amphiphiles belonging to different size ranges and at different stages of the cooling process. We show that, even though there is a high concentration of premicelles at τ_m, they are unstable and are constantly exchanging amphiphiles with the solution. This is in agreement with theoretical and experimental results, which have already suggested the rapid dissociation and association of surfactant molecules in the premicellar region. Even though eventually these premicelles are going to serve as nucleation sites to form larger aggregates, they have a transient nature and are quickly formed and dissolved until equilibrium is reached. We also observe that the mean lifetime of an amphiphile in a micelle is strongly influenced by the size of the latter, since this lifetime grows significantly with the aggregate size. Premicelles have an average lifetime which is 35 times shorter than large aggregates in equilibrium, which is also in agreement with the idea of large aggregates forming from unstable premicelles when we go from a nonmicellized to a micellized state. These results help explain the origin of the hysteresis we observe between the heating and cooling processes for the large temperature jumps, since they follow different paths towards equilibrium and that can be related to the amphiphile dissociation dynamics in each of them.

ACKNOWLEDGMENTS

The authors acknowledge the Brazilian agencies CNPq (Grants No. 2013/303253-4 and No. 2013/406863-0) and INCT-FCX (FAPESC-CNPq 537560/2008-0) for financial support.

[1] T. F. Tadros, *Surfactants* (Academic Press, London, 1985).
[2] J. N. Israelachvilli, *Intermolecular and Surface Forces* (Academic Press, London, 1992).
[3] R. Zana, ed., *Dynamics of Surfactant Self-Assemblies: Micelles, Microemulsions, Vesicles and Lyotropic Phases* (CRC Press, Boca Raton, FL, 2005).
[4] D. R. Karsa, *Industrial Applications of Surfactants* (Royal Society of Chemistry, London, 1988).
[5] C. Tanford, *Hydrophobic Effect: Formation of Micelles and Biological Membranes* (Wiley, New York, 1980).
[6] R. Pool and P. G. Bolhuis, J. Phys. Chem. B **109**, 6650 (2005).
[7] M. Girardi and W. Figueiredo, J. Chem. Phys. **112**, 4833 (2000).
[8] M. Girardi, V. B. Henriques, and W. Figueiredo, Chem. Phys. **328**, 139 (2006).
[9] D. J. Michel and D. J. Cleaver, J. Chem. Phys. **126**, 034506 (2007).
[10] M. Kenward and D. Whitmore, J. Chem. Phys. **116**, 3455 (2002).
[11] M. A. Floriano, E. Caponetti, and A. Z. Panagiotopoulos, Langmuir **15**, 3143 (1999).
[12] A. P. dos Santos, W. Figueiredo, and Y. Levin, Langmuir **30**, 4593 (2014).
[13] V. V. A. Fernandez, J. F. A. Soltero, J. E. Puig, and Y. Rharbi, J. Phys. Chem. B **113**, 3015 (2009).
[14] Y. Rharbi, L. Chen, and M. A. Winnik, J. Am. Chem. Soc. **126**, 6025 (2004).
[15] M. J. Kositza, G. D. Rees, A. Holzwarth, and J. F. Holzwarth, Langmuir **16**, 9035 (2000).
[16] M. J. Kositza, C. Bohne, P. Alexandridis, T. A. Hatton, and J. F. Holzwarth, Langmuir **15**, 322 (1999).
[17] C. Trachimow, L. De Maeyer, and U. Kaatze, J. Phys. Chem. B **102**, 4483 (1998).
[18] M. Li, Y. Rharbi, M. A. Winnik, and K. G. Hahn, J. Colloid Interface Sci. **240**, 284 (2001).
[19] R. Lund, L. Willner, M. Monkenbusch, P. Panine, T. Narayanan, J. Colmenero, and D. Richter, Phys. Rev. Lett. **102**, 188301 (2009).
[20] K. D. Danov, P. A. Kralchevsky, N. D. Denkov, K. P. Anantha-padmanabhan, and A. Lips, Adv. Colloid Interface Sci. **119**, 1 (2006).
[21] X. He and F. Schmid, Phys. Rev. Lett. **100**, 137802 (2008).
[22] R. Pool and P. G. Bolhuis, Phys. Rev. Lett. **97**, 018302 (2006).
[23] J. N. B. de Moraes and W. Figueiredo, Chem. Phys. Lett. **491**, 39 (2010).
[24] L. de Maeyer, C. Trachimow, and U. Kaatze, J. Phys. Chem. B **102**, 8024 (1998).
[25] D. N. LeBard, B. G. Levine, R. DeVane, W. Shinoda, and M. L. Klein, Chem. Phys. Lett. **522**, 38 (2012).
[26] J. N. B. de Moraes and W. Figueiredo, Phys. Rev. E **87**, 062315 (2013).
[27] F. K. Gottberg, K. A. Smith, and T. A. Hatton, J. Chem. Phys. **108**, 2232 (1998).
[28] E. A. G. Aniansson and S. N. Wall, J. Phys. Chem. **78**, 1024 (1974).
[29] E. A. G. Aniansson and S. N. Wall, J. Phys. Chem. **79**, 857 (1975).
[30] E. A. G. Aniansson, S. N. Wall, M. Almgren, H. Hoffman, I. Kielmann, and W. E. A. Ulbricht, J. Phys. Chem. **80**, 905 (1976).
[31] C. Tondre and R. Zana, J. Colloid Interface Sci. **66**, 544 (1978).
[32] E. Lessner, M. Teubner, and M. Kahlweit, J. Phys. Chem. **85**, 3167 (1981).
[33] G. Heinzelmann, W. Figueiredo, and M. Girardi, J. Chem. Phys. **131**, 144901 (2009).

[34] G. Heinzelmann, W. Figueiredo, and M. Girardi, J. Chem. Phys. **132**, 064905 (2010).
[35] G. Heinzelmann, W. Figueiredo, and M. Girardi, J. Chem. Phys. **134**, 064901 (2011).
[36] G. Heinzelmann, W. Figueiredo, and M. Girardi, Chem. Phys. Lett. **550**, 83 (2012).
[37] R. G. Larson, J. Chem. Phys. **96**, 7904 (1992).
[38] M. E. J. Newman and G. T. Barkema, *Monte Carlo Methods in Statistical Physics* (Clarendon Press, Oxford, 1998).
[39] D. Chandler, Nature **437**, 640 (2005).
[40] U. Kaatze, J. Phys. Chem. B **115**, 10470 (2011).